ASGE Vol. 06 (03), pp. 1-9, 2022

Egyptian Knowledge Bank

International Journal of Advances in Structural and Geotechnical Engineering

https://asge.journals.ekb.eg/

Print ISSN 2785-9509 Online ISSN 2812-5142

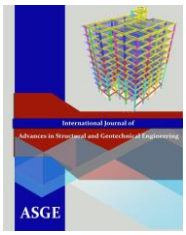

Experimental Study of High Strength Concrete T-Sections with Flange Openings

Ahmed Hassan[1], Fouad Khairallah[2] , Hala Mamdouh[3], Aya Mahmoud[4]

[1]*Professor, Faculty of Engineering, Beni-Suef University, Egypt*
E-mail: ahmedhb96@yahoo.com
[2,3]*Associate Professor, Faculty of Engineering, Helwan University, Egypt*
[2]*E-mail: fouad.khair@gmail.com*
[3]*E-mail: dr_hala_mamdoh@yahoo.com*
Teaching Assistant[4]*, Faculty of Engineering, Badr University in Cairo, Egypt*
E-mail: aya.mahmud@buc.edu.eg

ABSTRACT

Implementing a flange opening in the existing beam makes cracks surrounded the opening due to stress concentration, reduces beam stiffness, and alters the simple beam behavior to a more complex one. This paper shows the behavior of reinforced HSC T-sections with flange opening un-strengthened by additional reinforcement in the bending zone. For this purpose, six HSC beams divided into two groups were cast and tested. The tested beams were supported and loaded under a point load effect in the middle of the beam span. The studied parameters were flange opening number (without, single, and double) and main reinforcement ratio (μ). Cracking and failure loads were recorded; deflections at the position of mid-span were measured. The pattern of cracks and modes of failure were observed. It was found that decreasing the compression zone width by flange openings and increasing the main reinforcement ratio significantly affected cracking and maximum loads, a pattern of cracks, and maximum induced deflections and strains, i.e., bearing capacity and deformation capacity of such tested beams.

Keywords: T-sections, Flange Opening, Flexural Strength, Curvature.

1. INTRODUCTION

There are now several primary installations in the new building, such as heating, sanitation, and electricity. Therefore, many openings are needed in the floor slabs. At the construction stage, it is not possible to always decide the location of the openings. Sometimes, after the construction of the building has been completed, new slab openings are required at different locations for various reasons, for instance placement of new cables or other infrastructure [1]. Cutting the openings on existing slabs should be thoughtfully confronted and, if possible, avoided. When an opening is cut into an existing slab, the member's strength, energy dissipation, and ductility are significantly reduced. Consequently, the design codes recommend the necessity to study the structural elements before deciding on the size and locations of the slab openings for excess capacity and possible moment redistribution. They also advised avoiding cutting openings next to the beams because they may intersect the portion of the slab used as a T-beam. Several studies on the probability of using the concrete flange effect on flexural and shear strength were performed. They concluded that the concrete flange of T-sections contributes to increasing the ultimate shear and flexural strength compared to rectangular beams with the same web dimensions [2-4]. Researchers found that the flange reinforcement and the dimensions affect the flexural and shear strength of the T-sections significantly, and the ductility improved with the change in the width of the flange [5]. It is evident from previous studies how the flange effect improves the beam behavior. A reinforced concrete beam opening

causes many beam behavior problems, such as beam stiffness reduction, excessive cracking, excessive deflection, and beam strength reduction [6-8]. Furthermore, a sudden change in the beam's cross-sectional dimension resulted in high-stress in the opening corners, which resulted in inappropriate aesthetics and permanently cracking. The reduced rigidity of the beam could also cause excessive deflection of the load and lead to a substantial redistribution of internal forces and moments.

EXPERIMENTAL PROGRAM

Specimen Details

A total of six HSC beams with concrete compressive strength of fc' = 56 MPa divided into two groups. The first group (A) consists of three beams with the main reinforcement ratio of μ = 1.5% divided to one T-section beam without openings as a reference beam, a T-section beam with a single rectangular flange opening 180×360 mm at flexural zone from one side, and the remaining beam was provided with double rectangular flange opening 180×360 mm at flexural zone from both sides, as shown in Fig. 1. The second group (B) has the same details as a group (A), only the main reinforcement ratio (μ) changed to 4.6%, as shown in Table 1. To focus on the beams' flexural strength behavior and reduce the shear contributions, the shear span-depth (a/d) =3 [9].

Table 1: Properties of tested beams

Group	Specimen	μ (%)	*As*	b_w (mm)	t_s (mm)	*B* (mm)
A	T-1.5	1.5	2D16	120	75	600
	TS-1.5	1.5	2D16	120	75	600
	TD-1.5	1.5	2D16	120	75	600
B	T-4.6	4.6	2D18+2D22	120	75	600
	TS-4.6	4.6	2D18+2D22	120	75	600
	TD-4.6	4.6	2D18+2D22	120	75	600

Materials

In manufactured the test specimens, Table 2 presented the details of the concrete mix design. The used coarse aggregate was gravel with a nominal maximum size of 10 mm. The coarse and fine aggregate was mixed to achieve a well-graded aggregate. Ordinary Portland cement from the Al Arish factory was used, which matched the Egyptian Code ECP (203-2017) [10]. Ten percent by weight of the Portland cement was substituted by silica fume to increase the concrete strength and produce the target concrete compressive strength of 56 MPa. A superplasticizer (Type G) was used to enhance the concrete mix's workability using a low water/cementitious ratio, under the commercial name (Sikament ® - R 2004). Two types of steel For transverse reinforcement of reinforcement were used in manufactured beams for this work. diameters (6 mm), mild steel (characteristic yield strength of 240 MPa), were used for slab reinforcement, see Fig. 1. The main longitudinal reinforcement bars of diameters (10 mm and 16 mm), high-grade steel (characteristic yield strength of 400 MPa) were used. Reinforcement of each diameter was exposed to direct tension testing to obtain the actual mechanical properties.

Table 2: Concrete Mix Design Proportions (Kg/m^3)

Cement	Coarse Aggregate	Fine Aggregate	Silica Fume	Water	Superplasticizer
500	1050	677	55	160 Liter/m^3	11 Liter/m^3

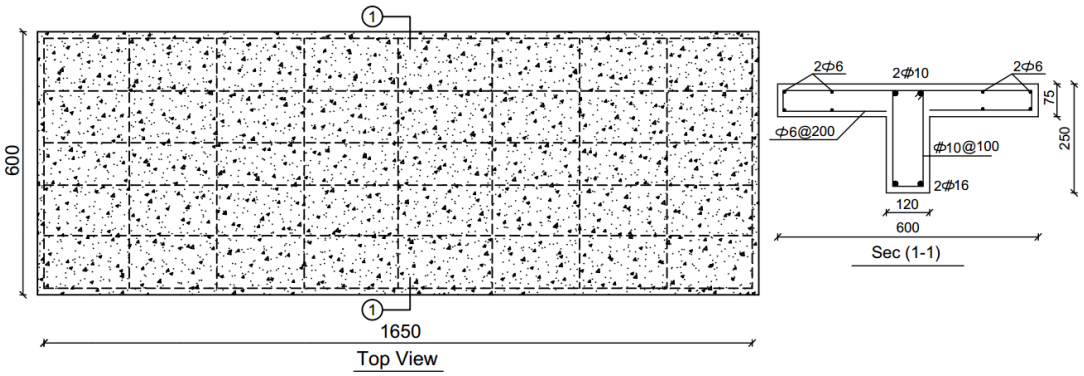

(a) Beam (T-1.5)

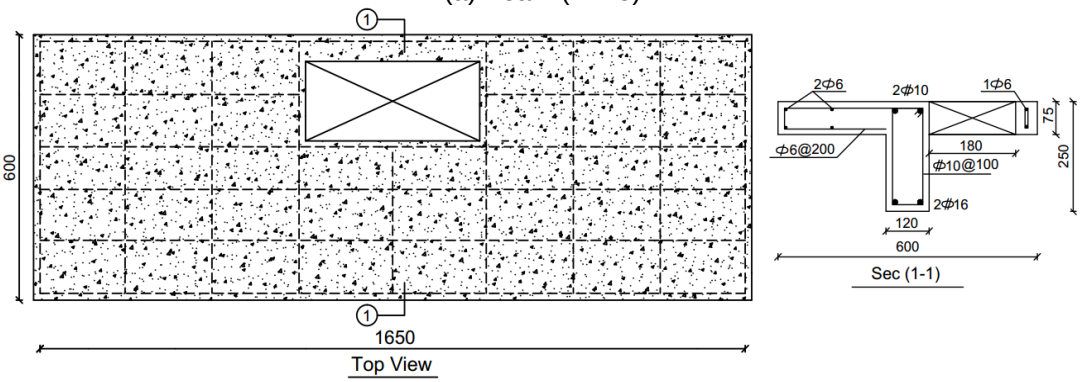

(b) Beam (TS-1.5)

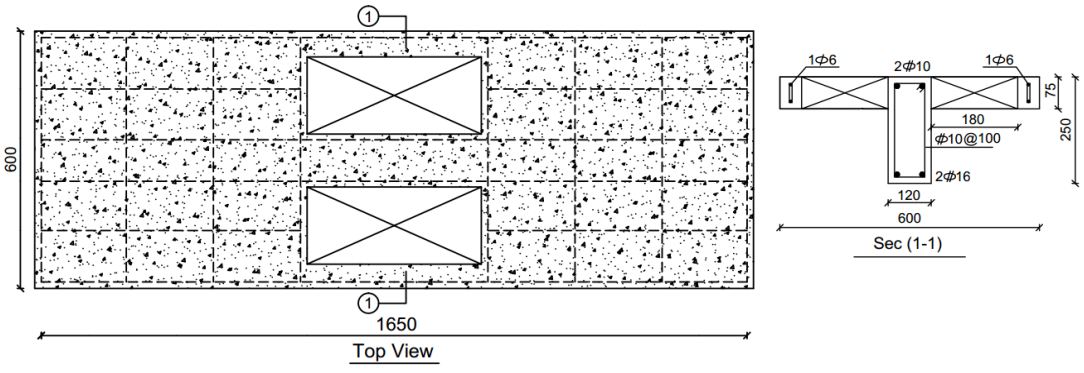

(c) Beam (TD-1.5)

Fig. 1: Details of Group (A) Specimens (unit. mm)

Instrumentation and Test Setup

After preparing the test setup and before loading, zero loadings of steel strain and vertical concrete displacements were recorded and checked. Three dial gauges were used to measure the vertical deflection of the beams. The first one was located at the middle of the span and others at a distance of 375 mm from the supports. The beam was tested as a single point loading system using a hydraulic jack attached to the loading frame, as shown in Fig. 2. The

beams have been tested at the ages of 28-days. The beam specimens were placed on the testing machine and adjusted so that the centerline, supports, point load, and dial gauges were in their correct location. Loading was applied slowly, at the end of each load increment, the crack initiation, path, and tip were outlined after the load had become steady, using a marker. The load was applied gradually with a constant rate of loading during the test. The measurement devices' readings were recorded in a paper sheet at every increment of load recorded by the load cell. The cracking load was recorded once the first crack was noticed. The crack pattern development was recorded after each load increment.

Fig. 2: Test Setup

EXPERIMENTAL RESULTS

Crack Pattern and Mode of Failure

Fig. 3 indicates that the flange openings do not significantly affect the crack pattern or change the control T-section's failure mode. The first cracks started in the constant moment region for the T-sections with and without flange openings and continued to spread as the applied load increased. The cracks then started to appear outside of the constant moment zone. At high applied load levels, no more flexural cracks were formed, but the existing cracks continued to widen as the beams increasingly deflected, and a few diagonal flexural shear cracks started in the shear regions. Before the failure, cracks continued from the web to the flange without crushing the flange until the beam failed. A ductile flexural failure occurred by yielding the tensile reinforcement after occurring large displacements. However, increasing the main reinforcement ratio by 206.7% directly affects the crack pattern but does not change the control T-section's failure mode. For the T-section with and without flange openings, few flexural cracks were initiated in the tested beams' mid-span at the early stages of loading. With additional loading, these cracks were spread upwards and widened in the shear region. One or more cracks spread faster than the others and reached the compression flange (nearly applied load or flange openings), where the crushing of the concrete near the applied load occurred due to high concentrated load stress and weak locations in the flange Finally, it can be concluded that decreasing the compression zone breadth (presence of flange openings) of HSC T-sections increased the cracks spacing, decrease the number of cracks in the flexural region, but the failure mode is still flexure.

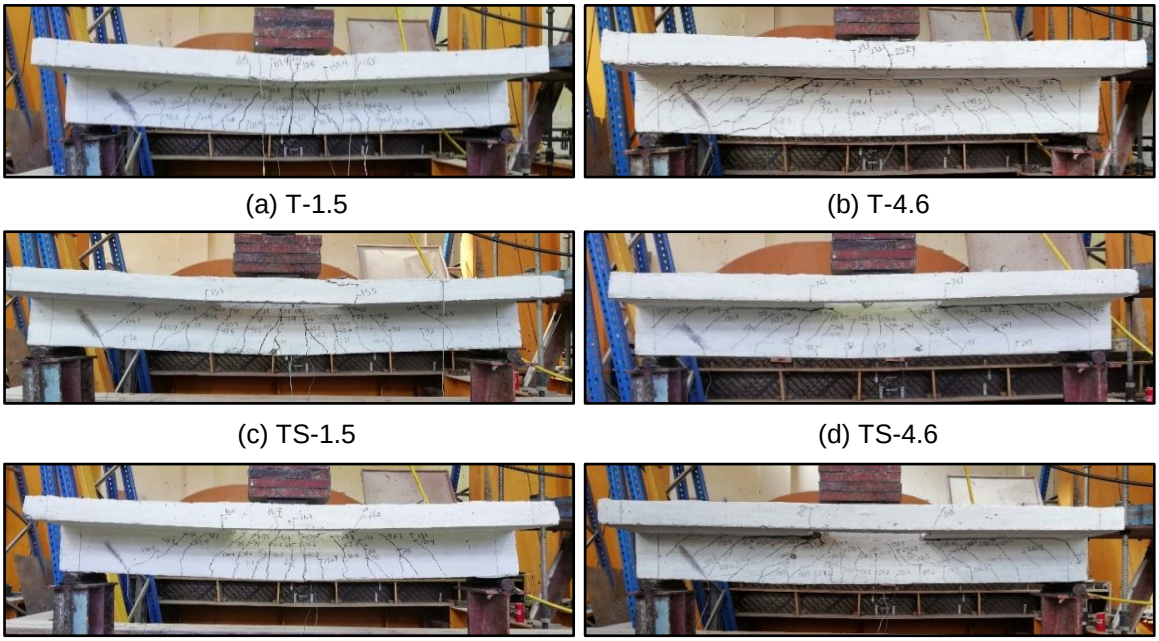

(a) T-1.5 (b) T-4.6

(c) TS-1.5 (d) TS-4.6

(e) TD-1.5 (f) TD-4.6

Fig. 3: Crack Pattern at Failure Stage of the Tested Beams

Moment Curvature

Curvature is a term that shows the structural deformation under the applied load [11]. In the mid-span section, the curvature was determined utilizing the experimental reinforcement strains and concrete strains, as per equation [1], and the neutral axis was calculated as per equation [2]. The numerical values are listed in Table 3

$$\varphi_u = \frac{\varepsilon_c}{c} \quad [1]$$

$$c = \frac{\varepsilon_c}{\varepsilon_c + \varepsilon_s} d \quad [2]$$

where φ is the beam curvature at a certain moment; ε_c is the concrete compressive strain at that moment; c is the distance from the extreme compression fiber to the neutral axis.

Table 3: Results of Energy-Based Ductility, Neutral Axis Depth and Curvature

Group	Specimen	μ_E (kN.mm)	$C_{Exp.}$ (mm)	φ (rad/mm)
A	T-1.5	2495.06	7.23	113.55
	TS-1.5	2376.47	7.89	146.26
	TD-1.5	2223.70	8.26	153.03
B	T-4.6	3882.99	40.20	44.45
	TS-4.6	2879.23	42.72	42.97
	TD-4.6	2444.14	48.80	38.34

Fig. 4 shows the moment-curvature curves for all tested beams, it can be noted that all beams exhibit similar moment-curvature behavior until the ultimate stage. In the ultimate stage, an

increase in the curvature of beams (TS-1.5) and (TD-1.5) was observed by comparing it with the beam (T-1.5). Where the ultimate curvature increased by about 28.86% and 34.83% for beams (TS-1.5) and (TD-1.5), respectively. The results indicated that the flange openings had a considerable effect on the curvature at the ultimate stage of HSC T-beams with a reinforcement ratio of 1.5%. By increasing the main reinforcement ratio as shown in Fig. 4b, it was found that all beams show similar moment-curvature behavior until the ultimate stage. In the ultimate stage, a slight reduction in the curvature of beams (TS-4.6) and (TD-4.6) was observed by comparing it with the control beam (T-4.6). Where the ultimate curvature decreased by about 3.33% and 13.75% for beams (TS-4.6) and (TD-4.6), respectively. But, the beams with flange openings had a higher curvature than the beam without flange openings at the same applied load. The results indicated that the flange openings had a little effect on the curvature at the ultimate stage of HSC T-sections with a reinforcement ratio of 4.6%.

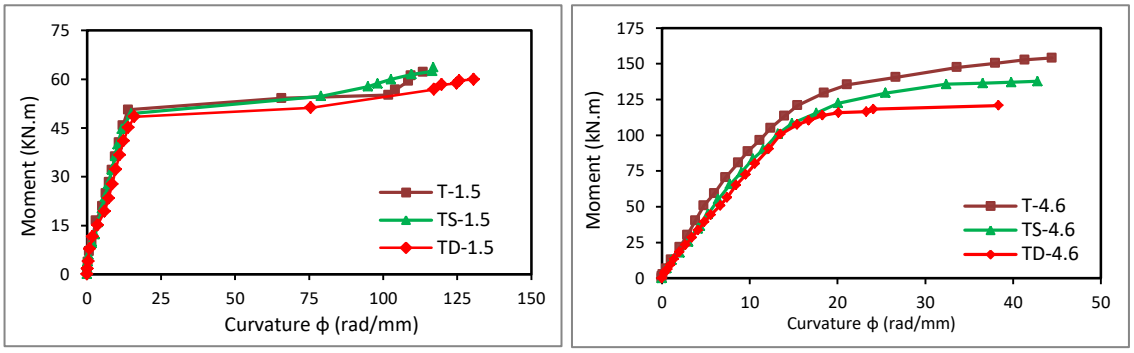

(a) Group (A) beams with μ = 1.5% (b) Group (B) beams with μ = 4.6%

Fig. 4: Moment-Curvature Curves

Ductility

Ductility is a desirable structural property because it allows stress redistribution and provides a warning of impending failure [12]. In this research, Energy-Based Ductility Method (μ_E) was explored, which is defined as the capacity of the beam energy absorption which is calculated using the area under the load-deflection curve up to the failure applied load [13]. The ductility indices of the tested beams based on energy concepts are listed in Table 4.

Fig. 5 shows that the slab openings had a minor effect on the energy absorption of reinforced HSC beams with the main reinforcement ratio of 1.5% as the energy-based ductility decreased by 4.8% and 10.91% for beams (TS-1.5) and (TD-1.5) respectively compared to the control beam (T-1.5). However, the slab openings had a substantial effect on the energy absorption of HSC beams with the main reinforcement ratio of 4.6%, where the energy-based ductility decreased by 25.85% and 37.06% for beams (TS-4.6) and (TD-4.6) respectively compared to beams (T-4.6).

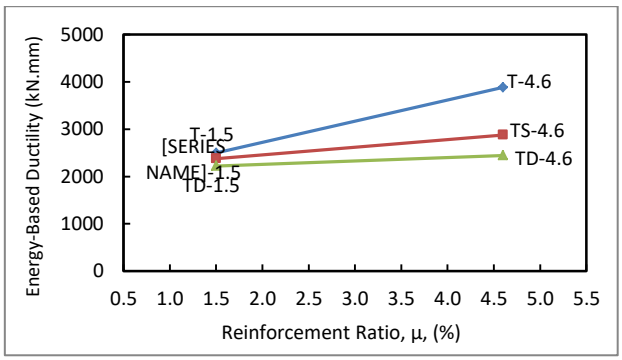

Fig. 5: Energy-Based Ductility Versus Main Reinforcement Ratio

Neutral Axis Depth

Fig. 6 shows the experimental neutral axis depth versus the applied load. The experimental neutral axis depth was calculated using equation [3] using the strain of the tensile reinforcement and the concrete compressive strain, which were measured from the experimental work. As shown in Fig. 6, the neutral axis depth tended to decrease after the flexural crack occurred. Subsequently, the neutral axis depth was maintained until tension reinforcement yield. After yielding the tension steel bars, the neutral axis (NA) depth greatly decreased. Some irregularities in the neutral axis depths (especially for beams with flange openings) occurred during loading due to the sensitivity of the strain gauge readings. The results also show that, for reinforced HSC beams with flange openings, the depth of NA at yield and the ultimate state has been increased. Similar observations were found by Sharifi and Maghsoudi [14].

$$c = \frac{\varepsilon_c}{\varepsilon_c + \varepsilon_s} d \qquad [3]$$

where c is the distance from the extreme compression fiber to the neutral axis in mm; ε_c is the ultimate concrete compressive strain; ε_s is the ultimate strain in the tension reinforcement; d is the distance from the centroid of the tension bars to the extreme compression fiber of the concrete beam in mm.

Fig. 6a shows that flange openings lead to a slight increase of the maximum neutral axis depth than the T-beams without flange openings for beams with the main reinforcement ratio of 1.5%. For example, the beam (T-1.5) had a maximum neutral axis depth of 7.23 mm at the load 173.31 kN while equal to 7.89 mm and 8.26 mm for the beams (TS-1.5) and (TD-1.5) at the load 169.74 kN and at the load 168.41 kN, respectively. Increasing the main reinforcement ratio to 4.6% for the same beams (TS-4.6) and (TD-4.6) led to an increase in the neutral axis depth by 6.27% and 21.39%, respectively, than the control beam (T-4.6) as shown in Fig. 6b.

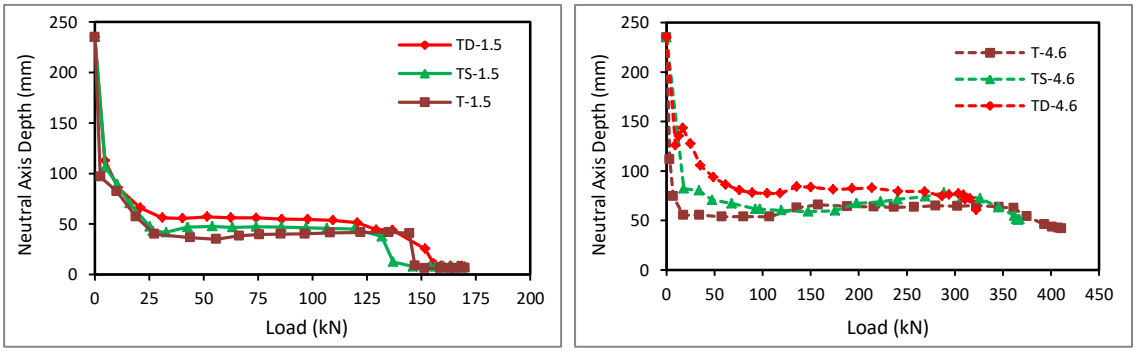

(a) Group (A) beams with μ = 1.5% (b) Group (B) beams with μ = 4.6%

Fig. 6: The Behavior of Neutral Axis Depth Under Load

CONCLUSION

This research studied the experimental behavior and flexural strength of HSC T-beams with slab openings. The following conclusions were drawn based on this study:

1. Flanges resulted in a general enhancement of the flexural behavior of tested beams as reflected by the increase in the ultimate load capacity, the increase in the pre-cracking and post-cracking stiffness, a reduction in the beam curvature, and deflection. Moreover, increasing the reinforcement ratio not only played a greater role in the pre-cracking stiffness of HSC T-beams but also improve their yielding and ultimate loads and reduce the overall deflection.

2. Flanges lead to a reduction of the maximum concrete strain at the compression zone. Thus, the tensile strain of reinforcement in T-sections are higher, and a higher position of the neutral axis is measured from the bottom of the beam. This indicates an increase in ductility with enlarging the flange breadth.

3. The creation of an opening in the flange of an existing beam leads to early diagonal cracking and significantly reduces the beam flexural capacity and stiffness.

4. The flange openings ratio in the range investigated here has no noticeable effect on the flexural behavior of the reinforced HSC T-sections with the main reinforcement ratio, μ = 1.5%. However, by increasing the main reinforcement ratio to 4.6%, the flange openings showed a considerable effect. In other words, the effect of the presence of flange openings on the behavior and strength of reinforced HSC T-sections becomes more remarkable as the percentage of main longitudinal steel ratio (μ) increases.

5. The flange openings had a significant effect on the curvature of HSC T-beams with the main reinforcement ratio of 1.5%. However, the flange openings had little influence on the curvature of HSC T-beams, with the main reinforcement ratio of 4.6%.

REFERENCES

1. H. Aziz and A. Ajeel, (2010), “Effect of Existing Flange Openings and Cold Joints on Strength of RC T-beams,” Journal of Engineering, Baghdad University, vol. 16 (1): pp. 4535-4546.

2. Giaccio C, Mahaidi RA and Taplin G, (2006), “Flange strain measurement in shear critical RC T-beams”, Advances in Structural Engineering, Vol. 9, No. 4, pp. 491–505.

3. Zararis LP, Karaveziroglou MK and Zararis PD, (2006), “Shear strength of reinforced concrete T-beams”. ACI Structural Journal, Vol. 103, No. 5, pp. 693–670.

4. Tureyen AK, Wolf TS and Frosch RJ, (2006), “Shear strength of reinforced concrete T-beams without transverse reinforcement”, ACI Structural Journal, Vol. 103, No. 5, pp. 656–663.

5. Shaaban, I. G., (2003), “Effect of Flange Characteristics on the Behaviour of High-Strength Concrete T-Beams,” Journal of the Egyptian Society of Engineers, Vol. 42, No. 2, pp. 13-24.

6. Said M. Allam, (2005), “Strengthening of RC beams with large openings in the shear zone,” Alexandria Engineering Journal, V.44, No.1, pp. 59 78.

7. M.A. Mansur, (1998), “Effect of Openings on the Behavior and Strength of R/C Beams in Shear,” Cement and Concrete Composites, V. 20, pp. 477-486.

8. Soroush Amiri, Reza Masoudnia and Ali Akbar Pabarja, (2011), “The Study of the Effects of Web Openings on the Concrete Beams,” Australian Journal of Basic and Applied Sciences, 5 (7): 547-556.

9. Li W. and Leung C. K.Y., (2016), “Shear Span–Depth Ratio Effect on Behavior of RC Beam Shear Strengthened with Full-Wrapping FRP Strip”, Journal of Composites for Construction, Vol. 20, No. 3, pp. 04015067-1-14.

10. ECP 203, (2017), “The Egyptian Building Code for Design and Construction of Reinforced Concrete Structures”, Ministry of Housing.

11. Omar I. Abdelkarim, Ehab A. Ahmed, Hamdy M. Mohamed & Brahim Benmokrane, (2019), “Flexural Strength and Serviceability Evaluation of Concrete Beams Reinforced with Deformed GFRP bars”, Engineering Structures, Vol. 186, pp. 282-296.

12. Withit Pansuk and Yasuhiko Sato, (2007), “Shear Mechanism of Reinforced Concrete T-Beams with Stirrups”, Journal of Advanced Concrete Technology, Vol. 5, No. 3, pp. 395-408.

13. Anas Yosefani, (2018), “Flexural Strength, Ductility, and Serviceability of Beams that Contain High-Strength Steel Reinforcement and High-Grade Concrete”, Ph.D. Thesis submitted to Portland State University.

14. Yasser Sharifi, Ali Akbar Maghsoudi, (2014), “An experimental study on the flexural behavior of heavily steel reinforced beams with high-strength concrete”, Front. Struct. Civ. Eng. 2014, 8(1): 46–56.